Characterization of the mechanical response of elastomers using complex experiments: Simple ways to describe multiaxiality

Léna Costecalde, Adrien Leygue, Michel Coret, Erwan Verron

Characterization of the mechanical response of elastomers using complex experiments:
simple ways to describe multiaxiality.

L. Costecalde, M. Coret, A. Leygue, E. Verron
Nantes Université, Ecole Centrale Nantes, CNRS, GeM, UMR 6183, 1 rue de la Noë, Nantes, 44321, France

ABSTRACT: Characterization of material response remains a challenging task. From the simultaneous use of simple experiments to multiaxial characterization with Finite Element Method Updating (FEMU) or Virtual Fields Method (VFM), several methods have been explored through the years. Thus, the possibility to characterize a material using only one "rich" experiment has made its path. As an example, the use of a multi-actuators machine, such as an Hexapod platform capable of 6-degrees freedom motions, can be considered as it allows a wide range of complex loading conditions.
The present paper aims to discuss the development of a rich mechanical experiment that guarantees a robust mechanical characterization by material parameters fitting or Data-Driven methods. A first approach consists in exhibiting the diversity of strain mulitaxiality and intensity thanks to Hencky's tensor invariants K_2 and K_3 introduced by Criscione, Humphrey, Douglas, & Hunter (2000). A second one is based on the strain energy density, in the hyperelastic framework. Here, complex tests are conducted on hyperelastic membranes. Strain maps of both multiaxiality and intensity are computed along the loading path. Comparison with the classical experimental data of Treloar (1944) is proposed.

1 INTRODUCTION

1.1 *Identification of mechanical response*

Through the years, methods have been developed to overtake the challenge of characterizing the mechanical response of materials. Constitutive equations, relating stress to strain by means of various derivatives and material parameters, are the most classical way to describe material response. For a given constitutive equation, identifying the best parameters to fit the mechanical response constitutes a real challenge. In this section, the classical material characterization technique is recalled, then two more advanced methods, based on complex tests, are described.

1.1.1 *Identification with simple deformation*

In continuum mechanics, strain and stress are represented by tensors, constituted of six components each. Constitutive equations are tensorial equations that are all the more simpler if tensors contain null components. The classical identification technique of mechanical response is based on this statement; Verron (2018) described such an identification process as using standard tests that guarantees simple deformation states with a direct calculation of stress tensors thanks to experimentally measured features: geometry of the sample, stretch, resulting force...
For elastomers, three classical mechanical tests are usually considered:

- Uniaxial tension (UT) on dogbone sample,
- Planar tension (PT) on long rectangular thin sample,
- Equibiaxial tension (EQT) on planar cross sample or by membrane out-of-plane inflation.

The corresponding experimental results are often combined to fit the parameters of a chosen constitutive equation with standard distance minimization processes. This identification method is summarized in Figure 1.

This classical method is largely used, whereas the amount of tests needed can be time and/or money consuming. Moreover, the simple deformation states are not always sufficient to characterize the whole mechanical response of a material, particularly in the case of complex loading conditions. This limitation motivates the development of more advanced identification methods based on complex experiments.

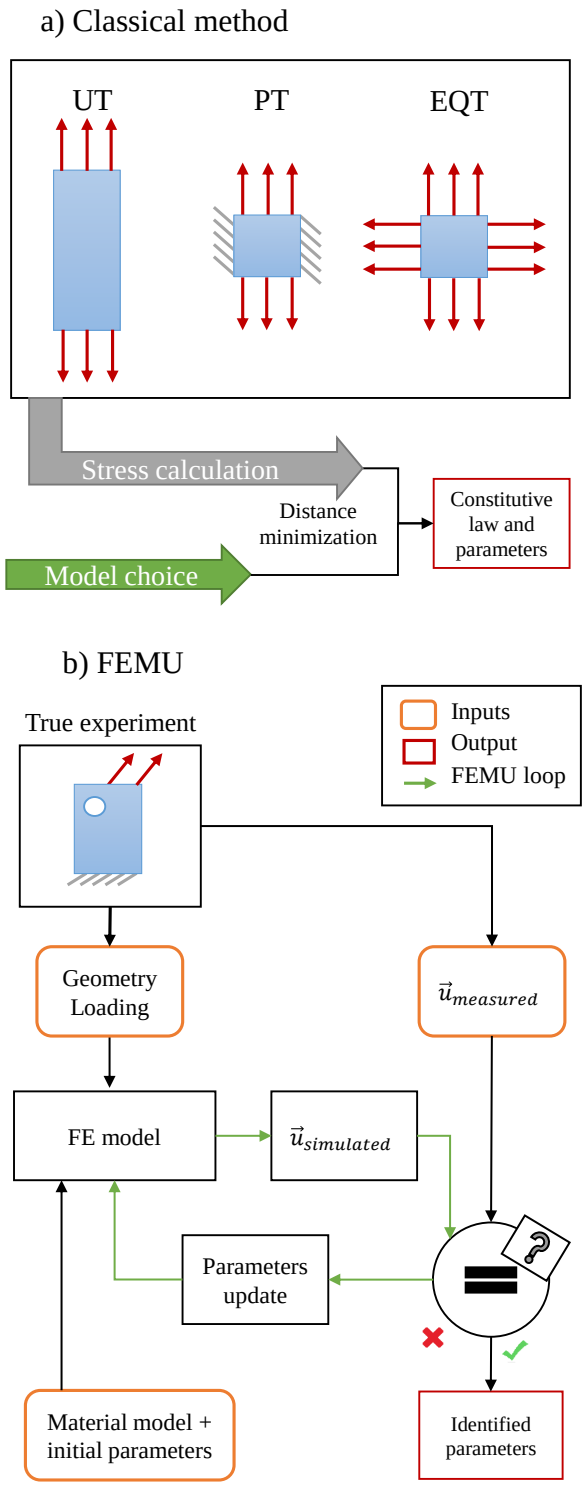

Figure 1: Identification methods for constitutive equations.

1.1.2 *Identification based on complex experiments*

In this section, two identification methods based on complex experiments are presented: Finite Element Model Updating (FEMU) described by (Ienny P. 2021) and Virtual Fields Method (VFM) described by (Jones, Karlson, & Reu 2019).

Finite Elements Updating Method is a numerical iterative method based on finite element simulation for the identification of parameters with complex tests. The method is described in Figure 1. Prior to the identification process, a constitutive equation and a starting set of parameters must be chosen. Resulting forces and displacements measured during the experiment are used as the algorithm's inputs, i.e. to define the boundary conditions of the finite element simulation . The difference between experimental and numerical displacement fields is calculated: if it exceeds the error tolerance, the algorithm iterates with a new set of parameters. The FEMU technique is well-adapted to complex tests, but also to anisotropic materials under simple loading conditions.

The Virtual Fields Method is an inverse method that aims to identify model parameters from measured full fields data, such as Digital Image Correlation results. The method is based on the Principle of Virtual Work, applied to a body submitted to finite deformation under plane stress conditions. The method follows this path at each iterative step:

- measurement of both full-field strain and resulting forces,
- computation of the stress field according to a given constitutive equation thanks to the strain field and an initial set of parameters,
- measurement or calculation of the thickness distribution,
- choice of a kinematically admissible virtual velocity field,
- computation of the error between internal and external virtual work, then optimization of the cost function.

This method has been proposed by Grediac, Pierron, Avril, & Toussaint (2006) for homogeneous, isotropic and linear elastic materials. Researchers have improved this method to study anisotropic and/or heterogenous and/or elasto-plastic and/or viscoelastic materials and/or viscoplastic materials (see for example (Jones, Karlson, & Reu 2019)).

To conclude, FEMU and VFM are two identification methods based on the results of multiaxial experiments. They necessitate less sample geometries and loading conditions than the above-mentioned classical simple deformation method. Nevertheless, they involve the choice of a given constitutive equation before the fitting computations.

1.2 *Present framework*

Here, the focus is laid on elastomer membranes, considered hyperelastic, submitted to complex loading conditions thanks to a multi-actuators machine. The material is assumed incompressible; samples are plane membranes, perforated or not. The corresponding experiments are design to adapt to the Digital Image Correlation technique in order to gather appropriate experimental data.

2 METHODS

A complex experimental test is the association of a sample, with defined geometry and material, and a loading path. In this section, theoretical ways to describe the complexity of deformation states are investigated, then two distinct strategies for developing such complex tests are proposed:

- "creating complexity" with perforated membrane and uniaxial tension,
- "creating complexity" with perforated membrane and complex loading paths.

2.1 *Deformation mode and intensity*

Among the variety of strain tensors, one of them generalizes the infinitesimal strain tensor to large strain: the Hencky (logarithmic) tensor. It is defined from the polar decomposition of the deformation gradient $\mathbf{F}$ and is sometimes referred to as the "true strain" tensor. It is defined as follows:

$$\mathbf{H} = \ln(\mathbf{V}), \text{ with } \mathbf{F} = \mathbf{VR}, \tag{1}$$

where $\mathbf{V}$ is the left pure strain tensor and $\mathbf{R}$ is the rotation tensor.

$\mathbf{H}$ can be described with the help of three well-chosen invariants, K_1, K_2, K_3 defined by Criscione, Humphrey, Douglas, & Hunter (2000) as indicators respectively of the "amount-of-dilatation", the "magnitude-of-distortion" and the "mode-of-distortion". They are defined as follows:

$$\begin{cases} K_1 = \text{tr}(\mathbf{H}) \\ K_2 = \sqrt{\text{dev}(\mathbf{H}) : \text{dev}(\mathbf{H})} \\ K_3 = \dfrac{3\sqrt{6}}{{K_2}^3}\det(\text{dev }(\mathbf{H})), \end{cases} \tag{2}$$

with

$$\text{dev}(\bullet) = \bullet - \text{tr}\left(\frac{\bullet}{3}\right)\mathbf{I}. \tag{3}$$

These invariants are used to describe deformation states. In this study, we only consider incompressible materials, then $K_1 = 0$. Thus, our description of deformation states only rely on K_2 and K_3. Thanks to incompressibility, the invariants become:

K_3	**Loading conditions**
1	Simple tension
0	Pure shear
-1	Simple compression or equibiaxial tension

Table 1: Particular values of K_3 and corresponding loading conditions.

$$\begin{cases} K_2 = \sqrt{\mathbf{H} : \mathbf{H}} \\ K_3 = \dfrac{3\sqrt{6}}{{K_2}^3}\det(\mathbf{H}). \end{cases} \tag{4}$$

K_2 is a real positive number that increases with the strain magnitude. K_3 is a real number between -1 and 1. Three particular values of K_3 are highlighted in Table 1. Any value between 0 and 1 describes a intermediate loading between uniaxial tension and pure shear, and any value between -1 and 0 describes an intermediate strain mode between simple compression and pure shear.

In the following, these two indicators will be calculated in each finite element and at each time step of the experiment and/or simulation to gather information about local deformation state.

2.2 *Strain energy density*

The use of the Data-Driven Identification (DDI) method proposed by Leygue, Coret, Réthoré, Stainier, & Verron (2018) allows to identify stress field without prescribing a constitutive equation. This algorithm is applied to kinematic fields of a complex experiment to compute the stress fields throughout the test. Once the stress fields obtained and with the incompressibility assumption, the strain energy density can be calculated in each element at each time step of the test:

$$W = \int_0^t \sigma : \mathbf{D}\, dt, \text{ with } \mathbf{D} = \frac{1}{2}(\dot{\mathbf{F}}\mathbf{F}^{-1} + (\dot{\mathbf{F}}\mathbf{F}^{-1})^T). \tag{5}$$

In the following, strain energy density will be used to characterize the "richness" of complex experiments.

2.3 *Synthetic data generation*

Two sets of data have been generated using Abaqus CAE software. The first set is composed of 20 loading steps of uniaxial tension on a perforated membrane, with a maximal stretch of 200%. The sample is displayed in Figure 2, and the material model used for the finite elements simulation is a third order Ogden model (six terms), which coefficients were determined for Treloar (1944) experiments by Ogden (Ogden 1972). The mesh consists of 6108 triangular lin-

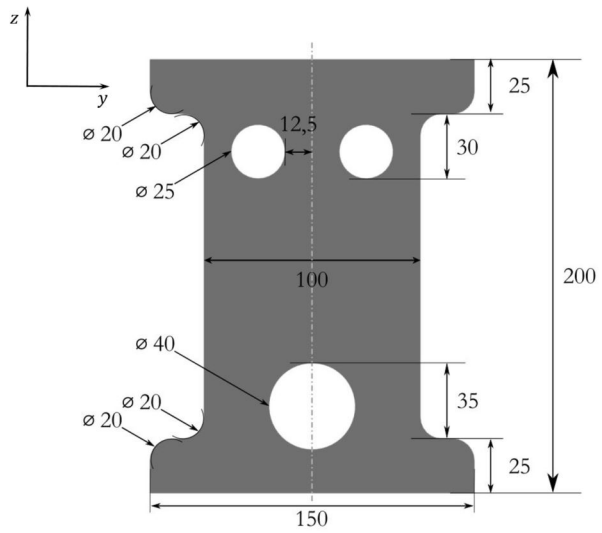

Figure 2: Perforated membrane for uniaxial tension test. The sample is referred as "3-holes membrane".

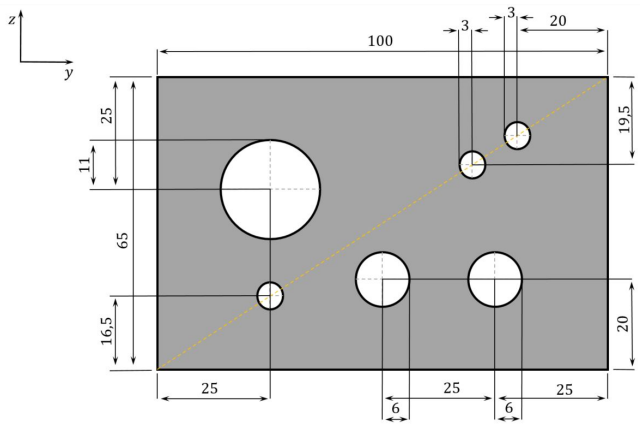

Figure 3: Perforated membrane geometry for complex test. The sample is referred as "6-holes membrane".

ear elements, and the displacements are prescribed on the top and bottom boundaries of the sample.

The second test involves a complex loading path applied to a perforated membrane. The sample is a 65 mm $\times$ 100 mm rectangular membrane with six holes from 3 to 22 mm diameter. The geometry is displayed in Figure 3. The upper edge of the sample remains fixed during the test, whereas the lower edge is submitted to six prescribed displacement step summarized in Table 2. The center of rotation is located in the middle of the bottom edge of the sample. The mesh is made of 2114 triangular linear elements, and the material considered incompressible, isotropic and linear elastic.

Step	u_y **(mm)**	u_z **(mm)**	R_x (°)
Initiale	0	0	0
Step 1	0	-20	0
Step 2	10	-20	0
Step 3	10	-20	12
Step 4	0	-30.40	12
Step 5	0	-40.79	0
Step 5	-10	-40.79	0

Table 2: Prescribed displacement steps of the complex loading path.

2.4 *Reference data*

A reference data set has been chosen to compare the magnitude and mode of distortion that are encountered during our complex tests.. Data from Treloar (1944) gather three types of tests:

- uniaxial tension,
- equibiaxial tension,
- and pure shear,

all applied to a vulcanized natural rubber. Hencky's tensor invariants K_2 and K_3 values have been calculated and will be compared to the results of the complex tests described above.

3 RESULTS

3.1 *Deformation states diversity in one loading step*

Figures 4 and 5 show the magnitude-of-distorsion and the mode-of-distorsion for each mesh element in the deformed configuration, respectively for the uniaxial and the complex loading path cases. The first one refers to the last step of the uniaxial tension test and the second one represents the fourth step of the complex loading experiment.

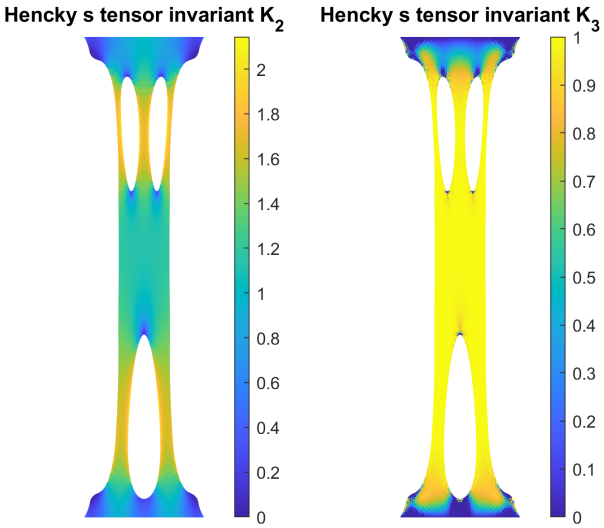

Figure 4: Magnitude-of-distorsion (left) and mode-of-distorsion (right) during the last loading step of the uniaxial tension case.

First, the left hand-side of Figure 4 is addressing the diversity of distortion magnitude encountered during this time step. Invariant K_2 varies from 0 to 2.18. Second, the right hand-side plot shows a much more uniform invariant K_3 distribution: the majority of the elements are coloured in yellow, i.e. $K_3 \approx 1$, which means that they endure uniaxial tension. Finally, even though the geometry of the sample generates some diversity in the distortion magnitude, the use of a single

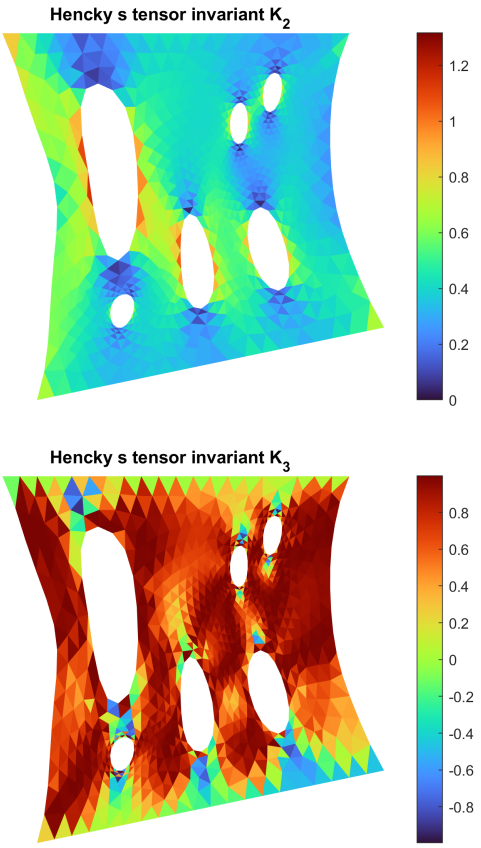

Figure 5: Magnitude-of-distorsion (top) and mode-of-distorsion (bottom) during the fourth step of the complex test on perforated membrane.

loading direction seems to induce a uniform mode of deformation throughout the sample.

Different observations can be made in Figure 5: a good diversity of distortion magnitude takes place (upper plot) even if it does not reach the previous experiment maximal "magnitude-of-distorsion" by kinematic construction of the test. Moreover, modes of deformation are also diverse as highlighted by colour map in the bottom plot. Various deformation modes from equibiaxial tension ($K_3 = -1$) to pure shear ($K_3 = 0$), then to uniaxial tension ($K_3 = 1$) and their intermediate states take place. It can be noted that despite its diversity, the major part of the the map is displaying orange to red tones: the corresponding finite elements are subjected to loading conditions close to uniaxial tension.

3.2 *Deformation states diversity through the experiment*

When considering a complex experiment made of various loading steps, the examination of unique K_2 and/or K_3 maps (for a given time step) is not sufficient to characterize the richness of the whole experiment. To overcome this difficulty, plots of Figure 6 are constructed.

Each map represents the distribution of the finite elements in the (K_2, K_3) plane during a given experiment. These maps are a little bit complex:

- Each pixel represents a deformation state, using a mode (K_3, along ordinate axis) and a magnitude (K_2, along the abscissa axis).
- The colour of the pixel corresponds to the proportion of elements that are in this deformation state during the experiment.
- The colour bar corresponds to the probability logarithm for an element taken randomly to be in this pixel of the map. The red and orange pixels correspond to a higher number of elements and the blue ones corresponds to a smaller one.
- Reference Treloar data are represented by small black crosses. They allows a comparison of the complex experiment with deformation modes and magnitudes classically used during the classical identification process.

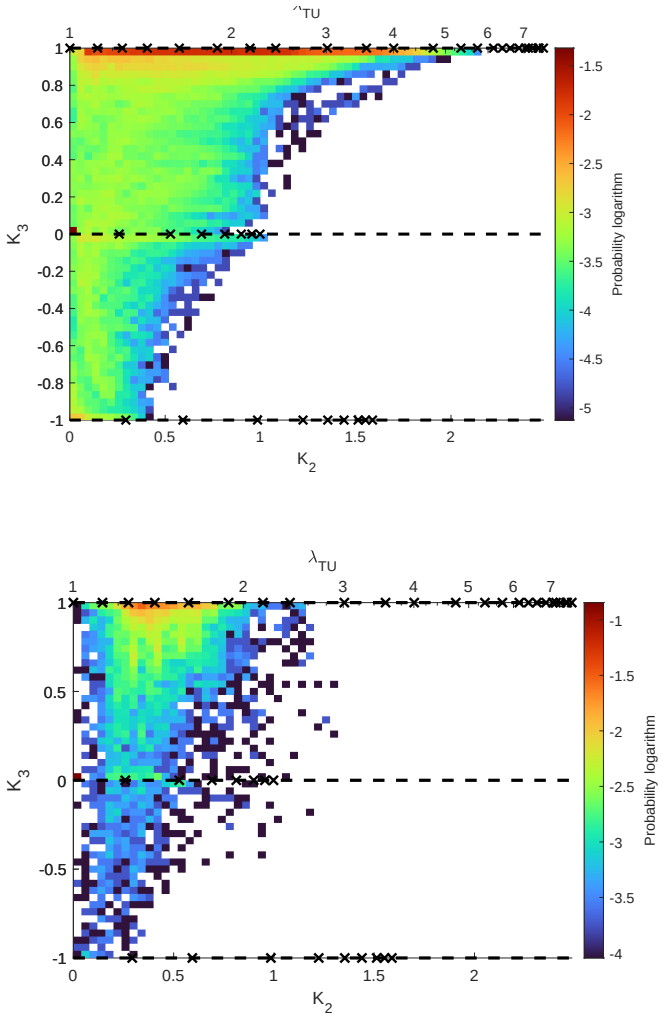

Figure 6: Deformation maps for the two experiments. Reference Treloar data are plotted using black crosses on the horizontal dotted lines corresponding to uniaxial tension ($K_3 = 1$), pure shear ($K_3 = 0$), and equibiaxial tension ($K_3 = -1$).
Top plot corresponds to uniaxial tension test on a 3-holes membrane. The 20 steps of the experiment are gathered.
Bottom plot corresponds to the complex experiment on a 6-holes membrane. The 6 loading steps of the experiment are gathered.

Figure 6, top plot, highlights a wide distribution of deformation modes during the experiment: at small strain ($K_2 \leq 0.4$), all deformation modes are attained

during the experiment. Moreover, the red line at the top of the map confirms the remarks for Figure 4: the majority of the finite elements are uniaxially stretched during this experiment. The deformation magnitudes corresponding to Treloar's data are reached for pure shear during this experiment, but neither for uniaxial tension nor equibiaxial tension.

Figure 6, bottom plot, also exhibits a wide distribution of deformation modes for small strain. The mode-of-distorsions that are exhibited by the complex test seem more spread vertically than in the previous test. The prescribed displacements are not sufficient to reach deformation magnitudes attained in the classical identification process, but the distribution of deformation modes is encouraging.

3.3 *Strain energy density diversity throughout the experiment*

The local strain energy density is an interesting feature that can be investigated during a complex test. Here, the distribution of strain energy density has been calculated from the stress field obtained by finite elements simulation. Its is depicted in the (K_2, K_3) plane as shown in Figure 7 for the 3-holes membrane under uniaxial tension.

We observe some strain energy density gradient along deformation magnitude axis: the strain energy density increases with the magnitude of deformation. Nevertheless, the (K_2, K_3) plane is not filled enough to allow to propose further conclusions. This part of the work is in progress.

4 CONCLUDING REMARKS

The use of Hencky's tensor invariants K_2 and K_3 defined by Criscione, Humphrey, Douglas, & Hunter (2000) allows a good characterization of deformation magnitude and mode under complex loading conditions. Assuming the incompressible nature of the considered materials, these two scalar quantities are sufficient to describe deformation states.

For a complex experiment, the distribution of these invariants can highlight the strain "richness" in a sample for a given loading state. Moreover, the map of finite elements density in the (K_2, K_3) space throughout a complex experiment is a relevant plot to characterize the "richness" of a given test. The strain energy density can be added to the map to expand the information.

In this study, the choice has been made not to develop any metric to summarize the maps. Metrics are scalar quantities used in comparison with a criterion, to evaluate a given property. Summarizing the (K_2, K_3) maps with for example the area covered by the point would have reduced the amount of information we can extract from the maps.

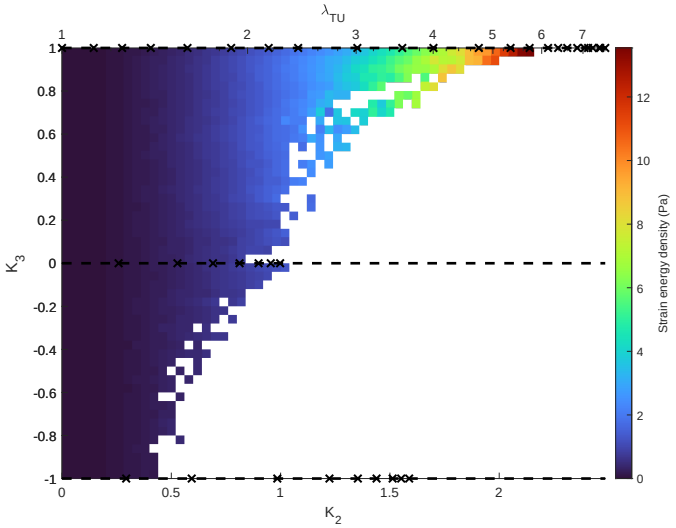

Figure 7: Strain energy density map in the (K_2, K_3) plane for the uniaxial tension of 3-holes membrane. Each pixel colour represents the average strain energy density of the finite elements with the corresponding pair (K_2, K_3).

REFERENCES

Criscione, J. C., J. D. Humphrey, A. S. Douglas, & W. C. Hunter (2000). An invariant basis for natural strain which yields orthogonal stress response terms in isotropic hyperelasticity. *Journal of the Mechanics and Physics of Solids 48*(12), 2445–2465.

Grediac, M., F. Pierron, S. Avril, & E. Toussaint (2006). The virtual fields method for extracting constitutive parameters from full-field measurements: a review. *Strain 42*(4), 233–253.

Ienny P., Caro-Bretelle A.S., P. E. (2021). Identification from measurements of mechanical fields by finite element model updating strategies. *Revue Européenne de Mécanique Numérique 353-376*.

Jones, E. M., K. N. Karlson, & P. L. Reu (2019). Investigation of assumptions and approximations in the virtual fields method for a viscoplastic material model. *Strain 55*(4), e12309.

Leygue, A., M. Coret, J. Réthoré, L. Stainier, & E. Verron (2018). Data-based derivation of material response. *Computer Methods in Applied Mechanics and Engineering 331*, 184–196.

Ogden, R. W. (1972). Large deformation isotropic elasticity–on the correlation of theory and experiment for incompressible rubberlike solids. *Proceedings of the Royal Society of London. A. Mathematical and Physical Sciences 326*(1567), 565–584.

Treloar, L. (1944). Stress-strain data for vulcanized rubber under various types of deformation. *Rubber Chemistry and Technology 17*(4), 813–825.

Verron, E. (2018). Modèles hyperélastiques pour le comportement mécanique des élastomères. *Techniques de l'Ingénieur AM 8 210*.